Cell, Vol. 110, 587–597, September 6, 2002, Copyright ©2002 by Cell Press

A Structural Mechanism of Integrin $\alpha_{IIb}\beta_3$ "Inside-Out" Activation as Regulated by Its Cytoplasmic Face

Olga Vinogradova,[1,2] Algirdas Velyvis,[1,2] Asta Velyviene,[1,2] Bin Hu,[2,3] Thomas A. Haas,[2,3] Edward F. Plow,[2,3,4] and Jun Qin[1,2,4]

[1]Structural Biology Program

[2]Department of Molecular Cardiology

[3]Joseph J. Jacobs Center for Thrombosis and Vascular Biology

Lerner Research Institute

The Cleveland Clinic Foundation

9500 Euclid Avenue

Cleveland, Ohio 44195

Summary

Activation of the ligand binding function of integrin heterodimers requires transmission of an "inside-out" signal from their small intracellular segments to their large extracellular domains. The structure of the cytoplasmic domain of a prototypic integrin $\alpha_{IIb}\beta_3$ has been solved by NMR and reveals multiple hydrophobic and electrostatic contacts within the membrane-proximal helices of its α and the β cytoplasmic tails. The interface interactions are disrupted by point mutations or the cytoskeletal protein talin that are known to activate the receptor. These results provide a structural mechanism by which a handshake between the α and the β cytoplasmic tails restrains the integrin in a resting state and unclasping of this interaction triggers the inside-out conformational signal that leads to receptor activation.

Introduction

Integrins are a major class of cell surface receptors that mediate cell-cell and cell-extracellular matrix interactions (Hynes, 1987, 1992; Schwartz et al., 1995; Giancotti and Ruoslahti, 1999). Such interactions play key roles in maintaining normal cellular functions and tissue integrity, and therefore, as evidenced by integrin deficiencies in humans (Caen et al., 1996; Anderson and Springer, 1987) or mice (Bouvard et al., 2001), these adhesion receptors are essential for development and/or health. Members of integrin family are noncovalent (α,β) heterodimers; each subunit consists of a single transmembrane domain, a large extracellular domain of several hundred amino acids, and typically, a small cytoplasmic tail of ~20–70 residues (Hynes, 1992). The extracellular domains form binding sites for numerous ligands, whereas the cytoplasmic domains anchor to the cytoskeletal and signaling proteins (Giancotti and Ruoslahti, 1999; Plow et al., 2000). In this manner, integrins link the exterior and interior of the cell, which is manifest in their regulation of cell adhesion, spreading, and migration.

Upon binding extracellular ligands, integrins transduce signals to the cytoplasm (outside-in signaling), which induces cascades of intracellular signaling events, including protein phosphorylation and cytoskeletal reorganization (Schwartz et al., 1995; Shattil and Ginsberg, 1997). However, ligand binding to integrins is not simply controlled by ligand availability but also through "inside-out" signaling: cellular stimulation clusters integrins or alters conformation to increase their avidity or affinity for ligands (Ginsberg et al., 1992; Shattil and Ginsberg, 1997; Hughes and Pfaff, 1998). The prototypic example of such integrin activation via inside-out signaling occurs with $\alpha_{IIb}\beta_3$. Platelets express $\alpha_{IIb}\beta_3$ on their surface, but only if the cells have been stimulated with an agonist that induces the appropriate inside-out signal does the receptor engage fibrinogen. Such inside-out regulation of $\alpha_{IIb}\beta_3$ affinity allows for rapid platelet aggregation to prevent excess bleeding while preventing uncontrolled receptor occupancy, resulting in thrombosis (Plow and Byzova, 1999).

As the trigger point of inside-out signaling, the integrin cytoplasmic face has been the focus of intense investigations (reviewed in Woodside et al., 2001). These studies have revealed that (1) while intact integrin can remain latent both in unstimulated cells and in a purified state, deletion of the cytoplasmic and transmembrane region activates the receptor (Peterson et al., 1998); (2) point mutations in the membrane-proximal regions of the cytoplasmic tails or deletion of either can result in constitutive activation of the receptor (O'Toole et al., 1994; Hughes et al., 1995, 1996); (3) replacement of the cytoplasmic-transmembrane regions by heterodimeric coiled-coil peptides or an artificial linkage of the tails inactivates the receptor, and breakage of the coiled-coil or clasp activates the receptor (Lu et al., 2001; Takagi et al., 2001); and (4) overexpression of certain intracellular proteins that bind to the cytoplasmic tails, including the cytoskeletal protein talin, which binds to the β cytoplasmic tail, can result in integrin activation (Eigenthaler et al., 1997; Calderwood et al., 1999; Tsuboi, 2002). These data suggest that a direct interaction between the α/β cytoplasmic tails might maintain the receptor in a latent state. However, vigorous biochemical/biophysical studies aimed at examining such interaction have yielded contradictory results. While certain studies have suggested such interactions (Haas and Plow, 1996; Vallar et al., 1999), recent NMR studies (Ulmer et al., 2001; Li et al., 2001) have failed to detect a complex. The most recent NMR study (Weljie et al., 2002) reported interaction between truncated versions of the α_{IIb} and β_3 cytoplasmic tail peptides, but structural analyses revealed two different complexes of unknown physiological relevance. Thus, our view of the cytoplasmic face and its regulation on the integrin inside-out signaling remains unclear, which is a major impediment to our understanding of integrin structure-function relationships.

In this study, we report the successful structure determination of the intact integrin $\alpha_{IIb}\beta_3$ cytoplasmic face using NMR spectroscopy. The structure reveals that the α_{IIb} and β_3 cytoplasmic tails do, indeed, interact; they engage in a weak handshake within their membrane-

[4]Correspondence: qinj@ccf.org (J.Q.), plowe@ccf.org (E.F.P.)

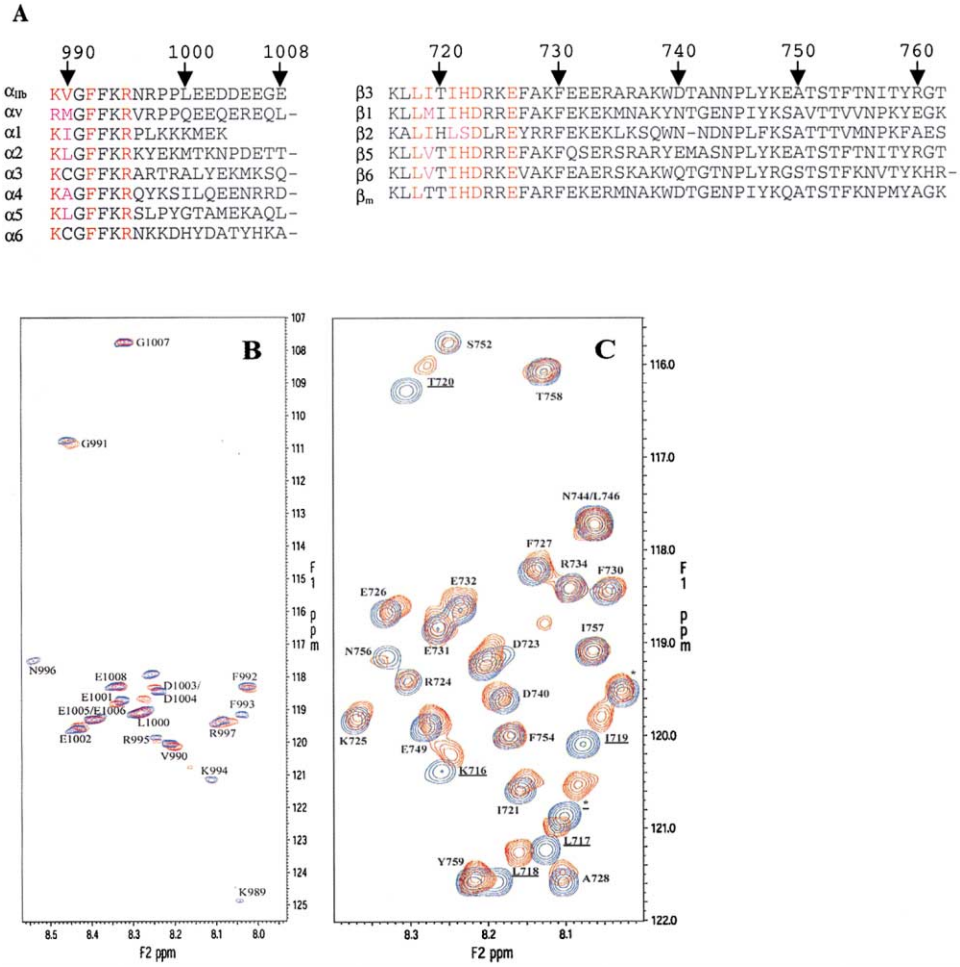

Figure 1. Sequences of Integrin α_{IIb}/β_3 Tails and Their Interaction

(A) Primary sequences of the α_{IIb} and β_3 tails and their alignment with other integrins. Highly conserved residues involved in the membrane-proximal interface are indicated by red (identical) and pink (similar).

(B) Expanded region of HSQC spectra of ^{15}N-labeled α_{IIb} in the absence (blue) and presence (red) of the unlabeled β_3 tail. Residue labels correspond to free α_{IIb} cytoplasmic tail.

(C) Expanded region of HSQC spectra of ^{15}N-labeled β_3 tail in the absence (blue) and presence (red) of the unlabeled α_{IIb} tail. Residue labels underlined indicate significant changes upon α_{IIb}/β_3 interaction. Asterisks indicate signals from His tag.

proximal regions. We further demonstrate that this handshake is unclasped by "activating" mutations (Hughes et al., 1996) in the binding interface and by a known integrin activator (Calderwood et al., 1999, 2002), the talin head domain. The results provide a structural basis for how an integrin cytoplasmic face regulates inside-out activation.

Results and Discussion

Detection of Interaction between the α_{IIb} and β_3 Cytoplasmic Tails by NMR

The sequences of the cytoplasmic tails of α_{IIb}, residues K989–E1008 (hereafter referred to as the α_{IIb} tail), and β_3, residues K716–T762 (the β_3 tail), are shown in Figure 1A. Although sequence analyses suggest secondary structure for the membrane-proximal regions of the tails, circular dichroism showed little helical content for the peptides in an aqueous environment (Haas and Plow, 1997). When the two tails were each fused to a coiled-coil helix, no interaction between them was detected in an aqueous environment by NMR, and they are unfolded except that the β_3 tail had a propensity to form an α helix in the N terminus and a turn at $N_{745}PLY_{748}$ motif (Ulmer et al., 2001). Nevertheless, when we examined the 2D ^{1}H-^{15}N heteronuclear single quantum correlation spectrum (HSQC) of the α_{IIb} tail (no fusion partner) in water, addition of unlabeled β_3 tail to the ^{15}N-labeled α_{IIb} tail led to small but reproducible chemical shift perturbations (Figure 1B). Consistent with CD studies (Haas and Plow, 1997), such chemical shift changes indicate that the β_3 tail influences the conformation of the α_{IIb} tail, suggesting formation of a complex. To verify this result, the inverse experiment was performed: the ^{15}N-labeled β_3 tail was mixed with the unlabeled α_{IIb} tail. Again, evidence for complex formation between the tails was noted by the change of HSQC spectrum of the β_3 tail (Figure 1C). Chemical shift changes as a function of the

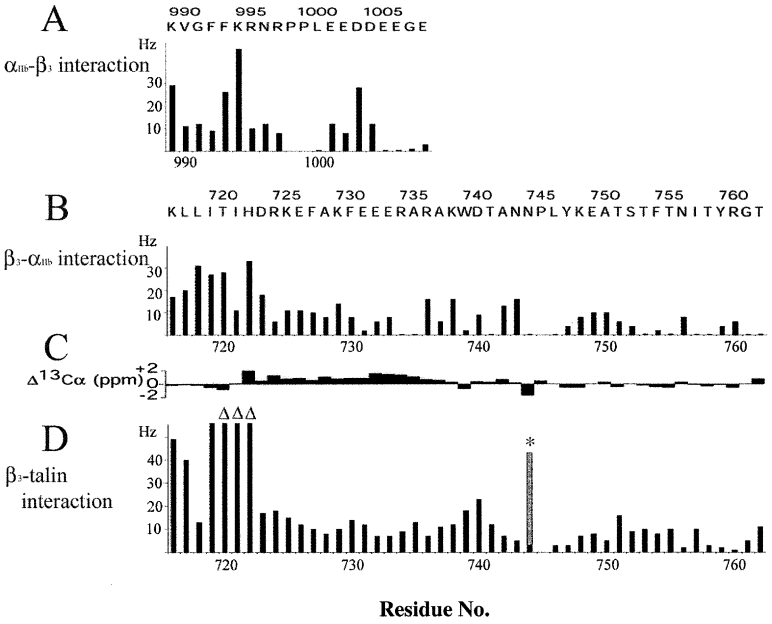

Figure 2. Summary of Spectral Perturbation for α_{IIb}/β_3 and β_3/Talin-H Interactions

(A) Chemical shift changes of the α_{IIb} tail upon binding to β_3 tail. The change of each residue was calculated based on a sum of absolute values of ^1H and ^{15}N chemical shift changes in Hz.

(B) Chemical shift changes of the β_3 tail upon binding to α_{IIb} tail.

(C) Difference between $^{13}C_\alpha$ shifts of each residue of the free β_3 tail in water and the corresponding random coil value. The large positive values of the C_α shift differences in the I721–A737 of the β_3 tail indicate that this region is predominantly α-helical (Spera and Bax, 1991). The helix is well defined upon binding to α_{IIb} (see the structure in Figure 4).

(D) Chemical shift changes for the β_3 tail upon binding to talin-H. The three-dot triangles for I719–T720 indicate that the signals underwent substantial change upon talin binding and disappeared due to either large chemical shift change or line broadening. The asterisk indicates the change of the N744 side chain.

residue number in the two cytoplasmic tails are summarized in Figures 2A and 2B. The significant changes in the α_{IIb} tail were detected in both the N-terminal K989–N996 and C-terminal E1001–D1004 regions, whereas the change in the β_3 tail was restricted to the N-terminal K716–D723. The small magnitude of the chemical shift changes may be due to the rapid reversibility and/or low affinity of the interaction (Vallar et al., 1999).

It is unclear why Ulmer et al. (2001) did not detect the weak interaction between the coiled-coil α_{IIb}/β_3 tail constructs that they used. Constructs in which the coiled-coils abut the membrane-proximal regions perturb conformation of the tails and reduce their binding to target proteins (Pfaff et al., 1998). Hence, any structural perturbation of the membrane-proximal regions may prevent weak interactions. In our study, we used either no fusion or flexible His tags at the N termini, which allowed detection of weak interactions. The interaction was further confirmed using additional constructs and additional NMR approaches (see below).

Approach to the Complete Structure Determination of the α_{IIb}/β_3 Cytoplasmic Complex

Although the free α_{IIb} and β_3 tails are soluble in water at mM concentration, the solubility of their complex was lower (<0.1 mM). The solubility of the α_{IIb}/β_3 tail mixture in detergent DPC micelles was higher (mM), which allowed for extensive NMR analyses of the individual tails (Vinogradova et al., 2000; O.V. and J.Q., unpublished data), but the micelles appeared to compete with the interaction of the tails. As a result, few intermolecular NOEs were observed for this system. A recent NMR study indicated that DPC induces a small curvature in α helices (Chou et al., 2002), and this subtle but nonnative structural alteration may perturb the weak α_{IIb}/β_3 tail interaction. Our results with DPC micelles are consistent with the recent study of Li et al. (2001), who also observed little interaction between α_{IIb}/β_3 tails in such micelles using constructs that included α_{IIb}/β_3 transmembrane domains and cytoplasmic tails. These peptides formed homooligomers in the detergent micelles. This propensity could play a role in integrin clustering.

To increase the solubility of the α_{IIb}/β_3 tail complex in water for structural determination, we explored several fusion constructs including those containing GST, Protein-G B1 domain (Zhou et al., 2001), and maltose binding protein (MBP) (Kapust and Waugh, 1999) as fusion partners. Of these, the highly soluble MBP substantially increased the solubility of the cytoplasmic tail complex into the mM concentration range. Moreover, direct intermolecular NOEs were observed between the two tails using this approach: see Figure 3A, in which $^{15}N/^{13}C$-labeled MBP-β_3 tail was mixed with unlabeled α_{IIb} tail, compared to Figure 3B, in which $^{15}N/^{13}C$-labeled MBP was mixed with unlabeled α_{IIb} tail. It is important to note that our MBP constructs had long linkers, which appear to exert little effect on the structural properties of the tails (Figure 3C) and their interaction (Figures 3A and 3E, see below). We were able to assign the resonances of the bound peptides based on 2D $^{14}N/^{12}C$-filtered NOESY and TOCSY (Ikura and Bax, 1992), which allowed structural analyses of the bound peptides and the intermolecular NOEs. Interestingly, since MBP fused to either the β_3 or α_{IIb} tail artificially increased the size of the weakly bound peptide complex, it was also feasible to perform high sensitivity transferred NOE experiments (Clore and Gronenborn, 1982; Campbell and Sykes, 1993) that provided valuable NOE constraints for structure calculations of the complex: Figure 3D displays the NOESY spectrum of 1 mM free α_{IIb} tail in water, which shows an unstructured pattern with only intraresidue and sequential NOEs. However, addition of 100 μM β_3 tail fused to the MBP (total MW ~48 kDa) resulted in a substantially increased number of NOEs, including medium- and long-range NOEs, indicating that the peptide becomes folded (Figure 3E). Apparently, the increased size of the complex allowed efficient NOE buildup as seen for high-molecular-weight molecules (>50

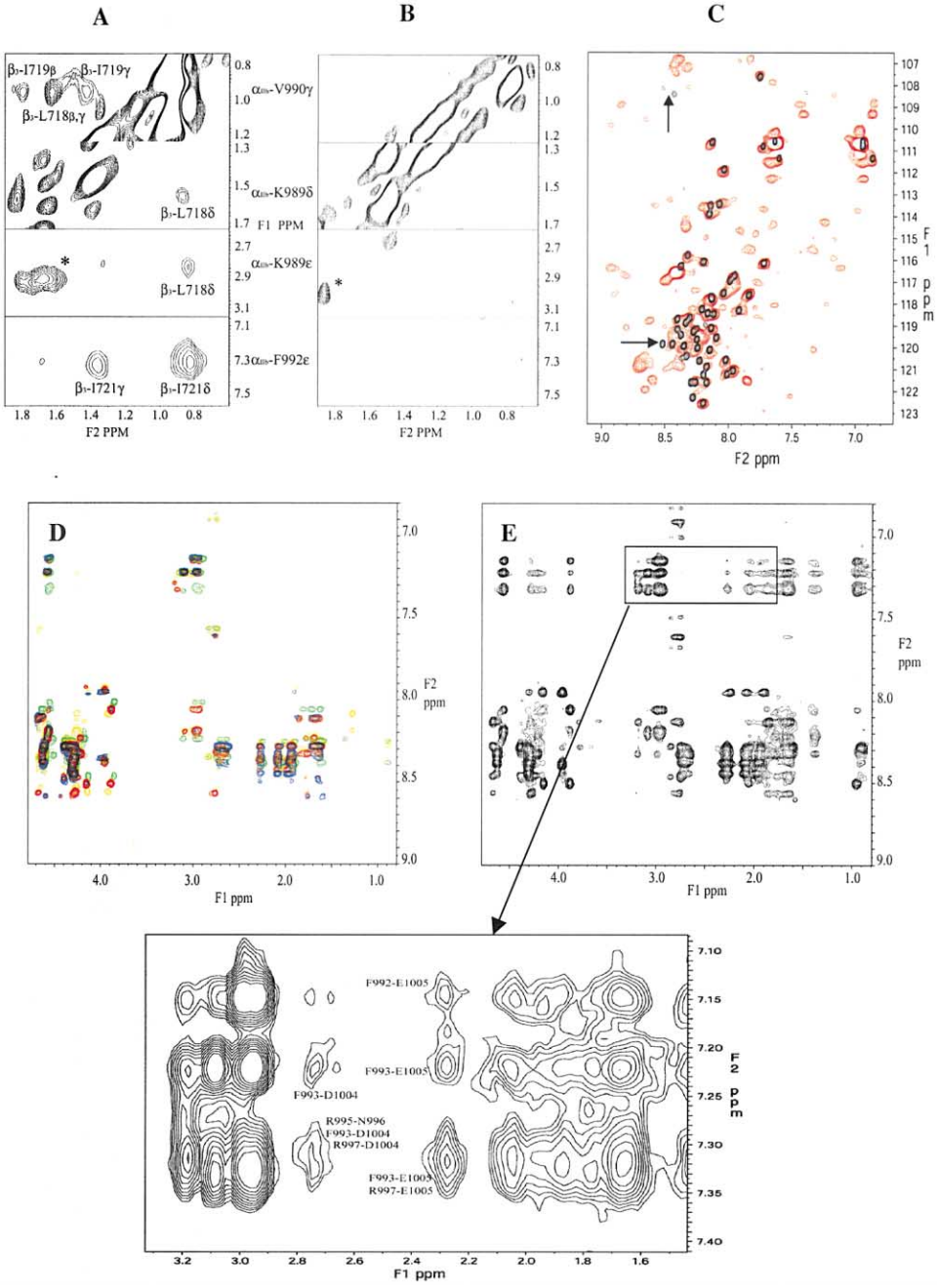

Figure 3. Spectroscopic Evidence for α_{IIb}/β_3 Tail Interaction

(A) Intermolecular NOEs between α_{IIb} and $^{15}N/^{13}C$-labeled β_3 tail fused to MBP (mixing time 250 ms). The asterisk peak appears to be the NOE between MBP and maltose ligand, which was also observed in the control experiment (see B).

(B) Control experiment showing no corresponding intermolecular NOEs between α_{IIb} and $^{15}N/^{13}C$-labeled MBP.

(C) Spectral overlay of HSQC spectra for β_3 cytoplasmic tail fused to His-tag (black) and β_3 cytoplasmic tail fused to MBP (red) collected at 500 Mhz, 25°C (pH 6.5). The signals of β_3 tail in both forms are essentially superimposable, although those from MBP-β_3 are much broader due to the large size of fusion MBP (42 kDa). Many signals from MBP are too broad to be observed at 25°C. Most of the signals from His-tag (20 aa) of β_3 cytoplasmic tail are exchanged with water at pH 6.5 and only a few of them are observed (indicated by arrows).

(D) 2D NOESY spectra of free α_{IIb} tail (red); α_{IIb} tail in the presence of MBP (blue, control experiment showing no transferred NOEs); α_{IIb} tail mutant (F992A) (orange); and α_{IIb} tail mutant (R992D) (green) in the presence of MBP-β_3 showing that the mutations diminished the transferred NOE effect. Slight chemical shift changes occur due to mutations.

(E) 2D NOESY spectrum of α_{IIb} tail in the presence of MBP-β_3. Substantial transferred NOEs appear as compared to (D), indicating that α_{IIb} tail is bound to β_3 tail fused to MBP. The zoomed region shows some long-range NOEs. The region was plotted at lower contour levels to reveal weak NOEs. Mixing time for each spectrum in (D) and (E) was 400 ms.

Table 1. Structural Statistics for α_{IIb}/β_3 Tail Complex

Parameter	SA Ensemble[a]
Rmsd from experimental distance restraints (Å)	
All (485)	0.073 ± 0.017
Intraresidue, i = j (229)	0.058 ± 0.014
Sequential, |i − j| = 1 (153)	0.074 ± 0.018
Medium range, 1 < |i − j| < 5 (65)	0.110 ± 0.026
Long range, |i − j| ≥ 5 (15)	0.017 ± 0.022
Intermolecular (13)	0.034 ± 0.045
Rmsd from idealized covalent geometry	
Bonds (Å)	0.005 ± 0.001
Angles (°)	0.62 ± 0.014
Impropers (°)	0.35 ± 0.009
E_{L-J} (kcal/mol)[b]	−156.17 ± 38
Ramachandran plot[c]	
Most favored regions (%)	75.0
Additionally and generously allowed regions (%)	25.0
Disallowed regions (%)	0.0
Coordinate precision[d]	
Rmsd of backbone atoms to the mean (Å)	0.87
Rmsd of all heavy atoms to the mean (Å)	1.51

[a] Mean ± standard error where applicable.
[b] Lennard-Jones potential energy function, calculated with CHARMM19 empirical energy parameters.
[c] Residues α_{IIb}(K989–E1008)/β_3(K716–T762). Total 20 SA structures.
[d] Residues α_{IIb}(K989–P999)/β_3(L718–K738) as shown in Figure 4B.

kDa) (Clore and Gronenborn, 1982; Campbell and Sykes, 1993). As a control, addition of MBP alone into the α_{IIb} tail had little effect on the NOESY spectrum of the free α_{IIb} tail (Figure 3D). Structure determination of the α_{IIb}/β_3 tail complex was performed based on a combination of the transferred NOEs, 2D $^{14}N/^{12}C$-filtered NOEs of the bound peptides, and intermolecular NOEs between the peptides (see Table 1 for structural statistics).

Overall Structure of the α_{IIb}/β_3 Cytoplasmic Complex

The superposition of the 20 best structures calculated for the α_{IIb}/β_3 tail complex is shown in Figure 4A. The structure of the α_{IIb} tail exhibits a helical feature in its N-terminal part (Figure 4B) that terminates at P998. This helix is followed by a turn, allowing the acidic C-terminal loop to fold back and interact with the positively charged N-terminal region. The bound α_{IIb} structure is quite similar to that of free α_{IIb} tail previously determined in DPC micelles (Vinogradova et al., 2000). The bound β_3 tail also exhibits α-helical structure in its N-terminal K716–K738 (Figure 4B). However, its C-terminal A737–T762 is disordered, consistent with the secondary structure analysis (Figure 2C). The C-terminal NPLY region appears to have propensity to form a turn, as reflected by the ^{13}C shift data (Figure 2C) and J_{HNHA} coupling constants (Ulmer et al., 2001); however, structure calculations did not reveal a well-defined turn in the aqueous condition used. The disordered C-terminal fragment of the β_3 tail is apparently not involved in binding to α_{IIb} since little spectral perturbation was observed in the presence or absence of the α_{IIb} tail (Figure 2B). Previous functional studies have shown that deletion of this C-terminal segment does not alter the activation state of $\alpha_{IIb}\beta_3$ (O'Toole et al., 1994; Calderwood et al., 1999). Hence, α_{IIb}(K989–E1008)/β_3(K716–K738) appears to form a functional cytoplasmic complex. The C-terminal segment of the β_3 tail likely

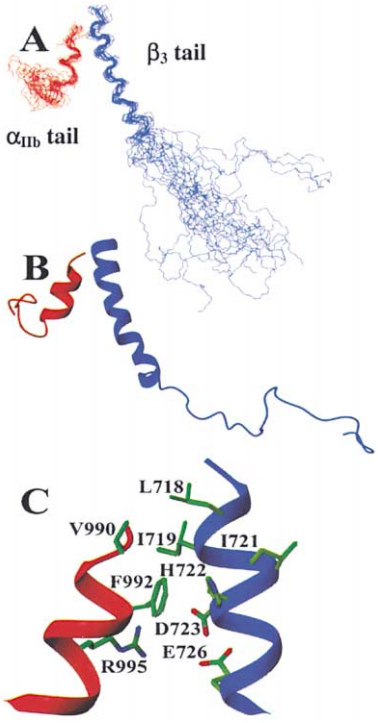

Figure 4. Structural Illustration of $\alpha_{IIb}\beta_3$ Tail Complex and Binding Interface

(A) Backbone superposition of 20 best structures of the α_{IIb}/β_3 tail complex.

(B) Backbone ribbon diagram of α_{IIb}/β_3 tail complex structure in the same view as (A). The figure was generated by the program MOLMOL (Koradi et al., 1996).

(C) Expanded view of the α_{IIb}/β_3 binding interface showing the hydrophobic and electrostatic interfaces.

acts as a docking site for the target proteins, e.g., β_3-endonexin (Eigenthaler et al., 1997), and may become folded upon binding to these proteins.

The primary interface between the α_{IIb} and β_3 tails is between their membrane-proximal helices (Figure 4C). The contacts are composed of a combination of hydrophobic and electrostatic interactions (Figure 4B). The hydrophobic interface mainly involves several methyl-containing residues and one phenylalanine: α_{IIb}(V990)-β_3(L718), α_{IIb}(V990)-β_3(I719), and α_{IIb}(F992)-β_3(I721). The α_{IIb} F992 aromatic ring also interacts with the β_3 H722 imidazole ring that is partially solvent exposed (Figure 4C). The electrostatic interface mainly involves side chains of the following pairs: α_{IIb}(R995 guanidyl group)-β_3(H722 imidazole group), α_{IIb}(R995 guanidyl group)-β_3(D723 carboxyl group), and α_{IIb}(R995 guanidyl group)-β_3(E726 carboxyl group). The interface pattern and sequence features do not strictly follow the rule of a typical two-stranded coiled-coil unit but do show some similarities, i.e., there is a hydrophobic core followed by the electrostatic interaction in the coiled-coil structure (Burkhard et al., 2001). The residues that mediate binding between the cytoplasmic tails are highly conserved in the integrin α and β subunits (Figure 1A), suggesting that that the interface, the resulting complex, and its functional consequences (see below) should be conserved across the integrins.

Role of the Cytoplasmic Interface in Controlling Integrin Activation

To evaluate the functional significance of the interface between the α_{IIb} and β_3 tails, we introduced two point mutations at residues in the α_{IIb} tail involved in formation of the α_{IIb}/β_3 complex. As shown in Figure 3D, a change of R995 to D in the α_{IIb} tail abolished the transferred NOE effect in the presence of MBP-β_3. Similarly, mutant α_{IIb} (F992A) also exhibited diminished transferred NOE effects (Figure 3D). Hence, disruption of either a representative hydrophobic or an electrostatic interaction involving F992 or R995, respectively, destabilized the cytoplasmic complex. Hughes et al. (1996) reported that either F992A or R995D mutations led to a constitutively active $\alpha_{IIb}\beta_3$. Hence, our data provide structural evidence that the α_{IIb}/β_3 tail interface maintains the receptor in the resting state, and disruption of the interface can initiate the inside-out signaling that culminates in activation. On this basis, we predict that other known constitutively activating mutations, such as α_{IIb} (F993A) (Hughes et al., 1996), α_{IIb} (P998A/P999A) (Leisner et al., 1999), and β_3 (D723A) (Hughes et al., 1996), may also perturb the α_{IIb}/β_3 interface either by directly disrupting the interface or by destabilizing the structures of the individual subunits. The α_{IIb} (P998A/P999A) mutant may be an example of the latter effect: although these proline residues are not directly in the binding interface between the tails, their mutations destabilize the α_{IIb} tail structure (Vinogradova et al., 2000).

With the above structural/mutational data strongly suggesting that unclasping of the cytoplasmic complex can be an initiating step for integrin inside-out signaling, we sought to determine if the mechanism is operational with a physiologically relevant activating stimulus, the cytoskeletal protein talin. Talin is a 250 kDa protein that is composed of a N-terminal head domain (talin-H, 1–435, 47 kDa) and a C-terminal rod domain (talin-R, 190 kDa) (Rees et al., 1990). Talin was first shown to bind to $\alpha_{IIb}\beta_3$ cytoplasmic face by Knezevic et al. (1996) and was more recently shown to activate $\alpha_{IIb}\beta_3$ by binding to the β_3 tail (Patil et al., 1999; Calderwood et al., 1999; Yan et al., 2001). Deletion and protease digestion experiments demonstrated that talin-H binds to the β_3 tail with high affinity ($K_D \sim 100$ nM) (Calderwood et al., 1999; Yan et al., 2001), and expression of this domain in heterologous cells leads to activation of $\alpha_{IIb}\beta_3$ (Calderwood et al., 1999). To establish the structural basis for direct talin-H/β_3 interaction in activating the $\alpha_{IIb}\beta_3$, we employed combined biochemical and structural approaches. First, we examined the activity of purified talin-H to activate purified $\alpha_{IIb}\beta_3$ using an immunocapture assay. Purified $\alpha_{IIb}\beta_3$ in a resting state was captured with a nonfunction blocking antibody onto microtiter wells in the absence or presence of various concentrations of talin-H. After an overnight incubation, ^{125}I-fibrinogen binding to the immunocaptured receptor was measured. In the absence of talin-H, fibrinogen binding to the $\alpha_{IIb}\beta_3$ was negligible. The talin-H domain induced concentration-dependent activation of the receptor such that fibrinogen bound to the captured $\alpha_{IIb}\beta_3$ (Figure 5A). In the absence of integrin, no binding of ^{125}I-fibrinogen to the antibody-coated wells in the presence or absence of talin was observed. The extent of fibrinogen binding induced by talin-H was substantially greater than that induced by RGD activation of the receptor, verifying that the purified talin-H was a potent activator of $\alpha_{IIb}\beta_3$. Also, as a control, the highest concentration of talin-H added to the wells was immobilized, and ^{125}I-fibrinogen binding to it was measured; the interaction was found to be only slightly greater than to immobilized bovine serum albumin and less than 10% of the binding to the immunocaptured receptor. Thus, the talin-H used in our subsequent structural studies could activate $\alpha_{IIb}\beta_3$.

Second, we used NMR to investigate structural details of the α_{IIb}/β_3/talin interaction. Unlabeled talin-H was added into either ^{15}N-labeled α_{IIb} tail or ^{15}N/70%^{2}H-labeled β_3 tail. While the talin-H addition had little effect on the HSQC spectrum of the α_{IIb} tail, it induced a significant perturbation in the β_3 tail spectrum (Figures 5B and 2D), demonstrating that talin-H specifically recognizes the β_3 tail, as consistent with the previous biochemical data (Patil et al., 1999; Calderwood et al., 1999; Yan et al., 2001). Significant chemical shift changes occur in two regions in the β_3 tail upon binding to talin-H (Figure 2D): (1) the membrane-proximal region involving K716–H722, which overlaps with the binding site for α_{IIb} tail (Figure 2D), and (2) the region N-terminal to NPLY motif involving W739–N744. Substantial line broadening occurs in the β_3 tail spectrum upon addition of the large talin-H binding, notably in the K716–D728 and A735–K748 regions. Our results are consistent with previous biochemical data that both membrane-proximal (Patil et al., 1999) and C-terminal NPLY region (Calderwood et al., 1999) are involved in binding to talin-H. Furthermore, synthetic peptides containing only N-terminal membrane-proximal K716–K738 or only C-terminal W739–T762 both bound weakly to a smaller ^{15}N-labeled talin-H fragment (183–429) (not shown), supporting the presence of the two talin binding sites in the β_3 tail. This

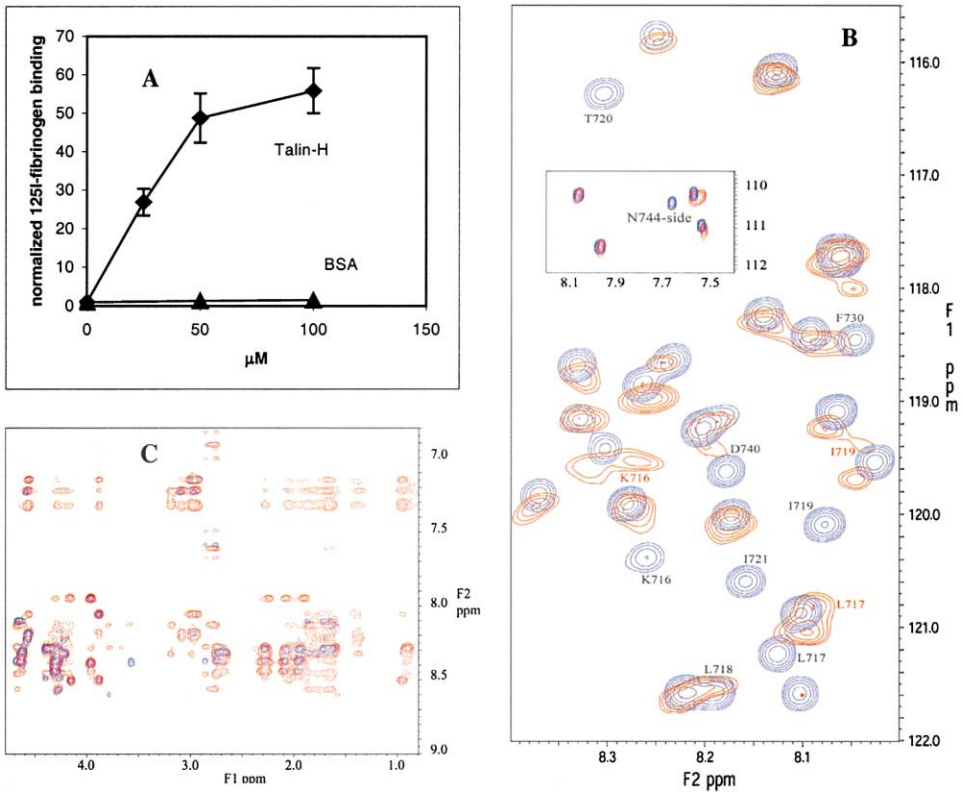

Figure 5. Talin-H Binds to the β_3 Tail and Activates $\alpha_{IIb}\beta_3$

(A) Talin-H activates purified $\alpha_{IIb}\beta_3$ in a dose-dependent manner. In contrast, the control protein BSA had little effect on the $\alpha_{IIb}\beta_3$ activation state. Talin and purified, resting $\alpha_{IIb}\beta_3$ (6.6 μg) were added to wells coated with mAb AP3 to the receptor. After an overnight incubation, the wells were washed, and ^{125}I-fibrinogen (300 nM) was added. After an additional 4 hr, the wells were washed and counted for radioactivity. The ^{125}I-fibrinogen binding to $\alpha_{IIb}\beta_3$ was normalized with the resting state integrin activity (no fibrinogen binding) as 1.0.

(B) Expanded region of HSQC spectrum of the ^{15}N-labeled β_3 in the absence (blue) and presence (red) of talin-H (see also Figure 2D). Substantial line broadening occurs due to the binding to large-sized talin-H. The inserted region denotes the side chain region showing perturbed N744 side chain.

(C) 2D NOESY of α_{IIb} tail in the presence of MBP-β_3 (red) and in the presence of both MBP-β_3 and talin-H (blue), showing that talin-H perturbs the α_{IIb}/β_3 tail interaction and abolishes the transferred NOE effect.

fragment of talin-H is sufficient to bind to the β_3 tail and to activate $\alpha_{IIb}\beta_3$ (Calderwood et al., 1999, 2002).

The overlapping binding site in the membrane-proximal region of the β_3 tail for α_{IIb} and talin-H (Figures 2B and 2D) suggested that talin-H might disrupt the α_{IIb}/β_3 tail complex leading to activation of the receptor. To test this hypothesis, we used two different approaches. (1) ^{15}N-labeled α_{IIb} tail was mixed with unlabeled β_3 tail and unlabeled talin-H. Examination of HSQC of the α_{IIb} tail in the mixture showed that its spectral pattern was the same as that for the free ^{15}N-lableled α_{IIb} shown in Figure 1B with no line broadening, indicating that no large ternary complex (α_{IIb}:β_3:talin-H) was formed and that the unlabeled β_3 tail in the presence of talin-H has little interaction with labeled α_{IIb} tail. Since the affinity of talin-H for β_3 tail (K_d ~100 nM) is substantially higher than that of α_{IIb} for β_3 (~7 μM) (Vallar et al., 1999), these data are consistent with disruption of the α_{IIb}/β_3 tail complex by the talin-H. (2) To provide independent demonstration of this mechanism, we again turned to the sensitive transferred NOE method, which allows detection of very weak protein-protein interactions. In contrast to the substantial transferred NOE effect observed for the α_{IIb}/MBP-β_3 mixture (Figure 5C), little transferred NOE effect was observed when talin was present (Figure 5C). These results strongly demonstrate that talin-H effectively competes with α_{IIb} tail for binding to β_3 tail, thereby disrupting the interaction between the two tails.

A Model for Regulation of Integrin Inside-Out Activation by the Cytoplasmic Domain

Using multiple NMR approaches, we have demonstrated that the α_{IIb} and β_3 tails interact with each other in an aqueous environment. Such an interaction had not been detected by Ulmer et al. (2001) or Li et al. (2001) but had been predicted and is key for understanding the integrin function. Further, we have been able to determine the solution structure of the heterodimeric complex. The structure revealed that the α_{IIb} and β_3 cytoplasmic tails interact with each other within their membrane-proximal helices via a combination of hydrophobic and electrostatic interactions. Although the α_{IIb} and β_3 tail interaction is relatively weak, such weak affinity is significant considering close proximity of the tails in the intact receptor and the multiple contacts between the α and β subunits in their extracellular regions (Xiong et al., 2001). Each

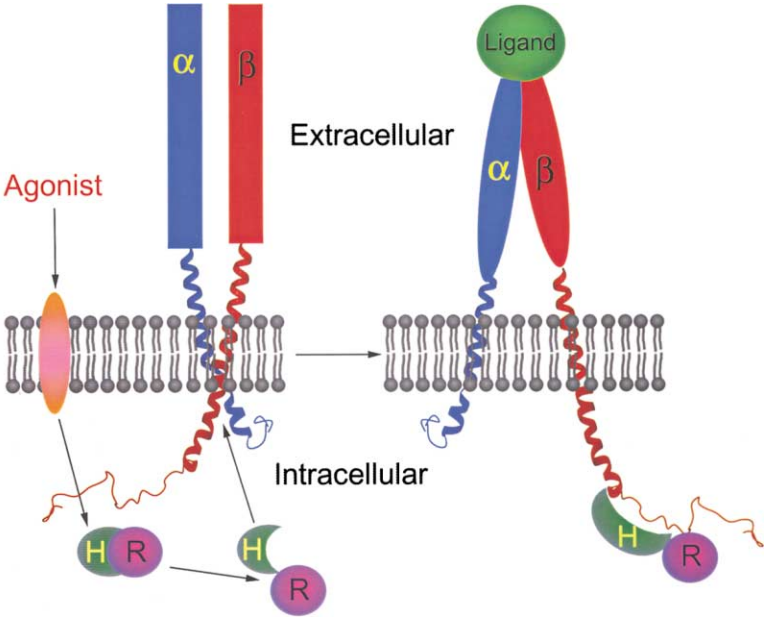

Figure 6. A Model for Talin-Induced Integrin Activation

Upon agonist stimulation, talin undergoes a conformational change that exposes the talin head domain and binds to the β_3 tail. The β_3/talin-H interaction displaces the α_{IIb}/β_3 tail interaction, leading to the opening of the C-terminal stalks and conformational rearrangement of the headpiece for high-affinity ligand binding. The α_{IIb}/β_3 transmembrane helices in the figure were extended manually from the structures of α_{IIb} and β_3 tails, respectively, by using InsightII program (Molecular Simulation, Inc.).

contact would enhance the overall affinity between the intact α_{IIb} and β_3 subunits. Indeed, deletion of the α_{IIb}/β_3 cytoplasmic-transmembrane fragments leads to lower efficiency of the α_{IIb}/β_3 heterodimerization (Frachet et al., 1992). Finally, we have structurally shown that this cytoplasmic tail interaction can be disrupted by a known integrin activator, talin-H, or by "activating" mutations, which suggests that unclasping of the cytoplasmic complex induces integrin inside-out activation. How this unclasping propagates the inside-out signal to the extracellular domain remains to be determined. Among the possibilities are: unclasping of the cytoplasmic tails may initiate a piston-like or scissor-like motion in the transmembrane helices, or cause a physical separation of specific contacts between the subunits, which induces a rearrangement of the extracellular headpiece for the ligand binding. This C-terminal separation model is supported by the elegant experiments by Lu et al. (2001) and Takagi et al. (2001) in which unclasping of artificial link between the C-terminal stalks activated the receptor. Our data appears to favor the model as shown in Figure 6: α_{IIb}/β_3 cytoplasmic interaction maintains the receptor in a low-affinity (inactive) state where the cytoplasmic tails engage in a weak handshake within their membrane proximal regions to form a "clasp." Upon agonist stimulation, a series of intracellular signaling events are initiated that culminate in disruption of the clasp. One of these signaling events may be induction of a conformational change in talin. This conformational change may be induced by phosphoinositides (Martel et al., 2001) or calpain cleavage (Yan et al., 2001) to expose the talin-H, which binds more effectively than intact talin to the β_3 tail and which displaces α_{IIb} tail from its complex with the β_3 cytoplasmic tail. The displacement of α_{IIb} releases the cytoplasmic constraint and opens up the integrin C-terminal stalks, which ultimately rearrange the extracellular headpiece for high-affinity ligand binding. This model is strongly supported by the above-mentioned point mutations/deletions (O'Toole et al., 1991, 1994; Hughes et al., 1996), which perturb the handshake between the α_{IIb} and β_3 tails and activate the receptor. Moreover, the cytoplasmic unclasping appears to release a structural constraint. Release of this constraint may directly initiate a conformation change that propagates across the membrane and activates the ligand binding function of the receptor or may allow receptors to cluster via homooligomerization of their transmembrane regions as suggested (Li et al., 2001), which further regulates integrin activation.

Since the regions involved in the handshake between the two subunits are conserved among the cytoplasmic tails of the integrin family, the model in Figure 6 for integrin activation is likely to apply broadly to the integrins. Also, while this particular scenario focuses on talin as the integrin activator, the mechanism implies that other molecules that interact with and disrupt the cytoplasmic complex would function as activators. Such interactions could arise through a competitive mechanism with the activator binding to the clasp region of either the α or β cytoplasmic tail, or they could arise through an allosteric mechanism, where the activators bind to the more C-terminal aspects of the tails and perturb the clasp. These alternative mechanisms for unclasping of α and β cytoplasmic tails are not merely speculative, since $\alpha_{IIb}\beta_3$ can be activated by two other intracellular molecules: calcium-and-integrin binding protein (CIB) (Tsuboi, 2002), which interacts with the α_{IIb} tail, and β_3-endonexin, which interacts with the C-terminal aspects of the β_3 tail (Eigenthaler et al., 1997).

While previous NMR studies had failed to detect the α_{IIb}/β_3 tail complex, Weljie et al. (2002) did report the structure of membrane-proximal portions of the α_{IIb} and β_3 cytoplasmic tails in complex using truncated fragments of each subunit. Comparison of the Weljie structure with ours reveals many substantial differences. (1) The Weljie structure is not uniquely defined; two alternative conformations of the β_3 membrane-proximal helix are present, and each has a severe bend in contrast to

our elongated structure. (2) More strikingly, the β_3 helices in both conformers are situated on the opposite side of the α_{IIb} N-terminal helix as compared to our structure of the complex. This orientation of the β_3 cytoplasmic tail would only appear to be possible in the absence of the α_{IIb} C terminus in their construct (with the intact α_{IIb}, its folded C terminus would clash with the β subunit and is therefore precluded). (3) Because of the difference in orientation, the key α_{IIb}/β_3 membrane-proximal interface in Weljie's structure is dramatically different from ours. Notably, α_{IIb}-F992 and α_{IIb}-R995 are critical in our structure by providing hydrophobic and electrostatic contacts with β_3 tail (Figure 4C), and these contacts provide an understanding of our mutational data (Figure 4D) and previous functional studies (Hughes et al., 1996). By contrast, both residues in Weljie structure are solvent exposed and point away from the β subunit. (4) Based on their data, Weljie et al. proposed a model for integrin activation in which the cytoplasmic tails remain complexed. In contrast, we propose that unclasping of the complex induces inside-out activation. This unclasping model appears to be more consistent with recent mutational studies (Lu et al., 2001; Takagi et al., 2001). Thus, while both studies detect a complex between the cytoplasmic tails, there are fundamental differences in the structures, which, in turn, lead to substantial differences in the models proposed for integrin activation.

Experimental Procedures

Expression and Purification of α_{IIb} and β_3 Tails

The cDNA of α_{IIb} tail was inserted into the pET31b vector (Novagen, Inc.) that expresses small peptides in *E. coli* into the inclusion bodies by fusing to an insoluble protein ketosteroid isomerase (KSI). Expression and purification of the peptide including the CNBr cleavage of KSI was performed according to the manufacturer's instructions (Novagen). The α_{IIb} tail was also subcloned into pMAL-c2x vector containing a N-terminal maltose binding protein (MBP) as the fusion (New England Biolabs, Inc.). The β_3 tail (K716–T762) was subcloned into pET15b (Novagen) and pMAL-c2x, respectively. The linker sequence for His tag of pET15b is GSS$(H)_6$SSGLVPRGSHM, which was CNBr cleavable, and the linker sequence for MBP and tails is S$(N)_{10}$LGIEGRISEFGS. Expression and purification of the α_{IIb} and β_3 tails each fused to MBP were performed according to the protocols from New England Biolabs, followed by gel-filtration. The β_3 tail encoded by pET15b was largely expressed in the inclusion bodies, and hence a denaturation-renaturation protocol (Novagen) was used for the purification followed by HPLC. The cDNA of talin-H (1–429) was subcloned into pET15b vector. The expression and purification procedures were the same as that for the β_3 tail encoded in pET15b except that purification was completed using a nondenaturation protocol (Novagen) followed by a gel filtration step. The talin-H was homogenous as assessed by SDS-PAGE.

Sample Preparation of Isotope-Labeled and Unlabeled α_{IIb} Tail, β_3 Tail, and α_{IIb}/β_3 Tail Complex

To make isotope-labeled α_{IIb} tail, β_3 tail, MBP-α_{IIb} tail, and MBP-β_3 tail, cells were grown in M9 minimal medium containing $^{15}NH_4Cl$ (1.1 g/l) and/or ^{13}C glucose (3 g/l) and/or ^2H_2O. Large quantities of unlabeled α_{IIb} tail, β_3 tail, β_3 K716–K738, and β_3 W739–T762 were also synthesized by our Biotechnology Core.

Samples for HSQC Titration Experiments

HSQC titration experiments in Figure 1 were performed by keeping the ^{15}N-labeled α_{IIb} at 80 μM mixed with 1–3 equivalent of unlabeled β_3 or vice versa. The sample conditions for examining HSQC of α_{IIb} tail/talin-H or β_3 tail/talin-H interactions were: unlabeled talin-H:^{15}N-labeled α_{IIb}= unlabeled talin-H:^{15}N/70%^2H labeled β_3 = 0.4 mM:0.2 mM = 2:1 in 20 mM phosphate buffer, 1 mM $CaCl_2$, 100 mM NaCl (pH 6.3). The sample conditions for examining talin-H interference on α_{IIb}/β_3 tail interaction were: ^{15}N-labeled α_{IIb}:unlabeled β_3 tail:unlabeled talin-H = 0.08 mM:0.10 mM:0.20 mM = 1:1.2:2.4.

Samples for Structural Analyses of the α_{IIb}/β_3 Tail Complex

To detect intermolecular NOEs and to analyze the structures of the unlabeled bound peptides, 1 mM $^{15}N/^{13}C$-labeled MBP-β_3 (or MBP-α_{IIb}) was mixed with 1.3 mM unlabeled α_{IIb} peptide (or β_3 peptide) in 20 mM phosphate buffer (pH 6.3), 5 mM Ca^{2+}. To examine the transferred NOE effect, a solution of 1 mM unlabeled α_{IIb} tail or mutants were prepared in the absence or presence of 0.1 mM MBP-β_3 in 20 mM phosphate buffer, 5 mM Ca^{2+} (pH 6.3). Similarly, a solution of 1 mM unlabeled β_3 (K716–K738) was prepared in the absence or presence of 0.1 mM MBP-α_{IIb} in 20 mM phosphate buffer, 5 mM Ca^{2+} (pH 6.3). To examine how talin-H perturbs the α_{IIb}/β_3 tail interaction using transferred NOE method, 1 mM unlabeled α_{IIb} tail was mixed with 0.1 mM MBP-β_3 and 0.2 mM talin-H in 20 mM phosphate buffer, 5 mM Ca^{2+} (pH 6.3). Note that previous studies revealed that divalent cations, including Ca^{2+} bound to the C-terminal of the α_{IIb} tail in a 1:1 stoichiometry, stabilizes the α/β complex (Haas and Plow, 1996; Vallar et al., 1999) and stabilizes the αIIb structure (Vinogradova et al., 2000). Hence, 5 mM Ca^{2+} was used to saturate or nearly saturate the 1 mM peptides.

NMR Spectroscopy

All heteronuclear NMR experiments were performed as described in Clore and Gronenborn (1998) and Ferentz and Wagner (2000). These experiments were performed at 25°C on Varian Inova 500 MHz spectrometer. The resonance assignments of free $^{15}N/^{13}C$-labeled α_{IIb} or β_3 peptide were made using standard triple resonance experiments. The resonance assignments of the unlabeled α_{IIb} (or β_3) peptide in complex with $^{15}N/^{13}C$-labeled MBP-β_3 (or MBP-α_{IIb}) were made using 2D $^{14}N/^{12}C$ filtered TOCSY and NOESY spectra (Ikura and Bax, 1992). These assignments were transferable to those in MBP-α_{IIb} or MBP-β_3 (Figure 3B). Intermolecular NOEs between the α_{IIb} and $^{15}N/^{13}C$-labeled MBP-β_3 or between $^{15}N/^{13}C$-labeled MBP-α_{IIb} and β_3 were obtained using 2D $^{15}N/^{13}C$ filtered (F1) NOESY (Zwahlen et al., 1997). Transferred NOESY experiments were performed with mixing times of 100 ms, 200 ms, 300 ms, and 400 ms to analyze NOE build-up in order to eliminate spin-diffusion artifacts. A control NOESY experiment (mixing time 400 ms) was always performed, e.g., on the 1 mM α_{IIb} tail mixed with 0.1 mM MBP (obtained by cleaving β_3 tail from MBP-β_3 followed by gel-filtration). DQF-COSY, TOCSY (mixing time 60 ms), and NOESY (mixing time 300 ms) were performed to assign resonances in both free and bound peptides using conventional 2D NMR method (Wüthrich, 1986). All the spectra were processed with nmrPipe (Delaglio et al., 1995) and visualized with Pipp (Garrett et al., 1991).

Structure Calculations

The structure of α_{IIb}-β_3 complex was calculated on a SGI Octane workstation using X-PLOR (Version 3.2) (Brunger, 1993). The individual subunit structures of α_{IIb} and β_3 tails were first calculated separately based on a combination of 2D $^{14}N/^{12}C$-filtered NOEs of the bound peptides and transferred NOEs. The complex was calculated afterwards by including intermolecular NOEs. The distance restraints were grouped into four distance ranges, 1.8–2.5 Å, 1.8–3.5 Å, 1.8–5.0 Å, and 1.8–6.0 Å, corresponding to strong, medium, weak, and very weak NOEs.

$\alpha_{IIb}\beta_3$ Purification and Activation by Talin

$\alpha_{IIb}\beta_3$ was purified in a resting state following the isolation procedure of Fitzgerald et al. (1985) except that fresh platelets were used as the starting material, 50 mM octyl-glucoside was used as the detergent to lyse the platelets, and 25 mM octyl-glucoside was used in the chromotographic steps. To assess fibrinogen binding to purified, resting $\alpha_{IIb}\beta_3$, an immunocapture assay was performed as previously described (Du et al., 1991; Vinogradova et al., 2000) using monoclonal antibody AP3 to bind receptor. Resting $\alpha_{IIb}\beta_3$ was captured overnight onto the AP3-coated surface in the absence or presence of different concentrations of talin-H. The binding buffer contained 10 mM HEPES (pH 7.4), 100 mM NaCl, 1 mM $CaCl_2$, 1 mM $MgCl_2$, 0.02% NaN_3, and 25 mM Octyl-glucoside. ^{125}I-fibrinogen (300 nM) was then added to the wells. The wells were incubated for

an additional 4 hr at room temperature and then washed. As a control, the RGDW peptide was used to induce activation of the immunocaptured receptor as previously described (Du et al., 1991).

Acknowledgments

We thank Frank Delaglio and Dan Garrett for NMR software; Drs. Gronenborn and Wagner for the constructs of protein G vectors; Joan Fox for the gift of cDNA constructs for talin-H, α_{IIb}, and β_3; and Yanwu Yang, Xiangming Kong, Fahima Rahman, Jing-yi Shi, and Jianmin Cui for assistance. The work was supported in parts by NIH grants to J.Q. and E.F.P. and AHA Scientist Development Grant to T.A.H. O.V. is supported by an NIH postdoctoral fellowship.

Received: April 26, 2002
Revised: August 1, 2002
Published online: August 31, 2002

References

Anderson, D.C., and Springer, T.A. (1987). Leukocyte adhesion deficiency: an inherited defect in the Mac-1, LFA-1, and p150,95 glycoproteins. Annu. Rev. Med. *38*, 175–194.

Bouvard, D., Brakebusch, C., Gustafsson, E., Aszodi, A., Bengtsson, T., Berna, A., and Fassler, R. (2001). Functional consequences of integrin gene mutations in mice. Circ. Res. *89*, 211–223.

Brunger, A.T. (1993). XPLOR Version 3.1 Manual (New Haven, CT: Yale University Press).

Burkhard, P., Stetefeld, J., and Strelkov, S.V. (2001). Coiled coils: a highly versatile protein folding motif. Trends Cell Biol. *11*, 82–88.

Caen, J.P., Leclerc, J.C., Inceman, S., Larrieu, M.J., Probst, M., and Bernard, J. (1996). Congenital bleeding disorders with long bleeding time and normal platelet count. I. Glanzmann's thrombasthenia. Am. J. Med. *41*, 2–26.

Calderwood, D.A., Zent, R., Grant, R., Rees, D.J., Hynes, R.O., and Ginsberg, M.H. (1999). The talin head domain binds to integrin beta subunit cytoplasmic tails and regulates integrin activation. J. Biol. Chem. *274*, 28071–28074.

Calderwood, D.A., Yan, B., de Pereda, J.M., Garcia-Alvarez, B., Fujioka, Y., Liddington, R.C., and Ginsberg, M.H. (2002). The phosphotyrosine binding (PTB)-like domain of talin activates integrins. J. Biol. Chem. *14*, 21749–21758.

Campbell, A.P., and Sykes, B.D. (1993). The two-dimensional transferred nuclear Overhauser effect: theory and practice. Annu. Rev. Biophys. Biomol. Struct. *22*, 99–122.

Chou, J.J., Kaufman, J.D., Stahl, J., Wingfield, P.T., and Bax, A. (2002). Micelle-induced curvature in a water-insoluble HIV-1 env peptide revealed by NMR dipolar coupling measurement in stretched polyacrylamide gel. J. Am. Chem. Soc. *124*, 2450–2451.

Clore, G.M., and Gronenborn, A.M. (1982). The two-dimensional transferred nuclear Overhauser effect. J. Magn. Reson. *48*, 402–417.

Clore, G.M., and Gronenborn, A.M. (1998). Determining the structures of large proteins and protein complexes by NMR. Trends Biotechnol. *16*, 22–34.

Delaglio, F., Grzesiek, S., Vuister, G.W., Zhu, G., Pfeifer, J., and Bax, A. (1995). NMRPipe: a multidimensional spectral processing system based on UNIX pipes. J. Biomol. NMR *6*, 277–293.

Du, X., Plow, E.F., Frelinger, A.L., III, O'Toole, T.E., Loftus, C., and Ginsberg, M.H. (1991). Ligands "activate" integrin $\alpha_{IIb}\beta_3$ (Platelet GPIIb-IIIa). Cell *65*, 409–416.

Eigenthaler, M., Hofferer, L., Shattil, S.J., and Ginsberg, M.H. (1997). A conserved sequence motif in the integrin beta3 cytoplasmic domain is required for its specific interaction with beta3-endonexin. J. Biol. Chem. *272*, 7693–7698.

Ferentz, A.E., and Wagner, G. (2000). NMR spectroscopy: a multifaceted approach to macromolecular structure. Q. Rev. Biophys. *33*, 29–65.

Fitzgerald, L.A., Leung, B., and Phillips, D.R. (1985). A method for purifying the platelet membrane glycoprotein IIb-IIIa complex. Anal. Biochem. *151*, 169–177.

Frachet, P., Duperray, A., Delachanal, E., and Marguerie, G. (1992). Role of the transmembrane and cytoplasmic domains in the assembly and surface exposure of the platelet integrin GPIIb/IIIa. Biochemistry *31*, 2408–2415.

Garrett, D.S., Powers, R., Gronenborn, A.M., and Clore, G.M. (1991). A common sense approach to peak picking in two- three- and four-dimensional spectra using automatic computer analysis of contour diagrams. J. Magn. Reson. *95*, 214–220.

Giancotti, F.G., and Ruoslahti, E. (1999). Integrin signaling. Science *285*, 1028–1032.

Ginsberg, M.H., Du, X., and Plow, E.F. (1992). Inside-out signaling. Curr. Opin. Cell Biol. *4*, 766–771.

Haas, T.A., and Plow, E.F. (1996). The cytoplasmic domain of $\alpha_{IIb}\beta_3$: a ternary complex of the integrin α and β subunits and a divalent cation. J. Biol. Chem. *271*, 6017–6026.

Haas, T.A., and Plow, E.F. (1997). Development of a structural model for the cytoplasmic domain of an integrin. Protein Eng. *10*, 1395–1405.

Hughes, P.E., and Pfaff, M. (1998). Integrin affinity modulation. Trends Cell Biol. *8*, 359–364.

Hughes, P.E., O'Toole, T.E., Ylanne, J., Shattil, S.J., and Ginsberg, M.H. (1995). The conserved membrane-proximal region of an integrin cytoplasmic domain specifies ligand binding affinity. J. Biol. Chem. *270*, 12411–12417.

Hughes, P.E., Diaz-Gonzalez, F., Leong, L., Wu, C., McDonald, J.A., Shattil, S.J., and Ginsberg, M.H. (1996). Breaking the integrin hinge. A defined structural constraint regulates integrin signaling. J. Biol. Chem. *271*, 6571–6574.

Hynes, R.O. (1987). Integrins: a family of cell surface receptors. Cell *48*, 549–550.

Hynes, R.O. (1992). Integrins: versatility, modulation, and signaling in cell adhesion. Cell *69*, 11–25.

Ikura, M., and Bax, A. (1992). Isotope-filtered 2D NMR of a protein-peptide complex: study of a skeletal muscle myosin light chain kinase fragment bound to calmodulin. J. Am. Chem. Soc. *114*, 2433–2440.

Kapust, R.B., and Waugh, D.S. (1999). *Escherichia coli* maltose-binding protein is uncommonly effective at promoting the solubility of polypeptides to which it is fused. Protein Sci. *8*, 1668–1674.

Knezevic, I., Leisner, T.M., and Lam, S.C.T. (1996). Direct binding of the platelet integrin $\alpha_{IIb}\beta_3$ (GPIIb- IIIa) to talin—evidence that interaction is mediated through the cytoplasmic domains of both α_{IIb} and β_3. J. Biol. Chem. *271*, 16416–16421.

Koradi, R., Billeter, M., and Wuthrich, K. (1996). MOLMOL: a program for display and analysis of macromolecular structures. J. Mol. Graph. *14*, 51–55.

Leisner, T.M., Wencel-Drake, J.D., Wang, W., and Lam, S.C. (1999). Bidirectional transmembrane modulation of integrin $\alpha_{IIb}\beta_3$ conformations. J. Biol. Chem. *274*, 12945–12949.

Li, R., Babu, C.R., Lear, J.D., Wand, A.J., Bennett, J.S., and DeGrado, W.F. (2001). Oligomerization of the integrin alphaIIbbeta3: roles of the transmembrane and cytoplasmic domains. Proc. Natl. Acad. Sci. USA *98*, 12462–12467.

Lu, C., Takagi, J., and Springer, T.A. (2001). Association of the membrane proximal regions of the alpha and beta subunit cytoplasmic domains constrains an integrin in the inactive state. J. Biol. Chem. *276*, 14642–14648.

Martel, V., Racaud-Sultan, C., Dupe, S., Marie, C., Paulhe, F., Galmiche, A., Block, M.R., and Albiges-Rizo, C. (2001). Conformation, localization, and integrin binding of talin depend on its interaction with phosphoinositides. J. Biol. Chem. *276*, 21217–21227.

O'Toole, T.E., Mandelman, D., Forsyth, J., Shattil, S.J., Plow, E.F., and Ginsberg, M.H. (1991). Modulation of the affinity of integrin alpha $_{IIb}$beta$_3$ (GPIIb-IIIa) by the cytoplasmic domain of alpha$_{IIb}$. Science *254*, 845–847.

O'Toole, T.E., Katagiri, Y., Faull, R.J., Peter, K., Tamura, R., Quaranta, V., Loftus, J.C., Shattil, S.J., and Ginsberg, M.H. (1994). Integrin cytoplasmic domains mediate inside-out signal transduction. J. Cell Biol. *124*, 1047–1059.

Patil, S., Jedsadayanmata, A., Wencel-Drake, J.D., Wang, W., Knezevic, I., and Lam, S.C. (1999). Identification of a talin-binding site in the integrin beta(3) subunit distinct from the NPLY regulatory motif of post-ligand binding functions. The talin N-terminal head domain interacts with the membrane-proximal region of the beta(3) cytoplasmic tail. J. Biol. Chem. *274*, 28575–28583.

Peterson, J.A., Visentin, G.P., Newman, P.J., and Aster, R.H. (1998). A recombinant soluble form of the integrin $\alpha_{IIb}\beta_3$ (GPIIb-IIIa) assumes an active, ligand-binding conformation and is recognized by GPIIb-IIIa specific monoclonal, allo-, auto-, and drug-dependent platelet antibodies. Blood *92*, 2053–2063.

Pfaff, M., Liu, S., Erle, D.J., and Ginsberg, M.H. (1998). Integrin beta cytoplasmic domains differentially bind to cytoskeletal proteins. J. Biol. Chem. *273*, 6104–6109.

Plow, E.F., and Byzova, T. (1999). The biology of glycoprotein IIb-IIIa. Coron. Artery Dis. *10*, 547–551.

Plow, E.F., Haas, T.A., Zhang, L., Loftus, J., and Smith, J.W. (2000). Ligand binding to integrins. J. Biol. Chem. *275*, 21785–21788.

Rees, D.J., Ades, S.E., Singer, S.J., and Hynes, R.O. (1990). Sequence and domain structure of talin. Nature *347*, 685–689.

Schwartz, M.A., Schaller, M.D., and Ginsberg, M.H. (1995). Integrins: emerging paradigms of signal transduction. Annu. Rev. Cell Biol. *11*, 549–599.

Shattil, S.J., and Ginsberg, M.H. (1997). Perspective series: cell adhesion in vascular biology. Integrin signaling in vascular biology. J. Clin. Invest. *100*, S91–S95.

Spera, S., and Bax, A. (1991). Correlations of C^{α}/C^{β} chemical shifts to the protein secondary structure. J. Am. Chem. Soc. *113*, 5490–5492.

Takagi, J., Erickson, H.P., and Springer, T.A. (2001). C-terminal opening mimics 'inside-out' activation of integrin alpha5beta1. Nat. Struct. Biol. *8*, 412–416.

Tsuboi, S. (2002). Calcium integrin-binding protein activates platelet integrin alphaIIb beta3. J. Biol. Chem. *277*, 1919–1923.

Ulmer, T.S., Yaspan, B., Ginsberg, M.H., and Campbell, I.D. (2001). NMR analysis of structure and dynamics of the cytosolic tails of integrin alphaIIb beta3 in aqueous solution. Biochemistry *40*, 7498–7508.

Vallar, L., Melchior, C., Plancon, S., Drobecq, H., Lippens, G., Regnault, V., and Kieffer, N. (1999). Divalent cations differentially regulate integrin α_{IIb} cytoplasmic tail binding to β_3 and to calcium- and integrin-binding protein. J. Biol. Chem. *274*, 17257–17266.

Vinogradova, O., Haas, T., Plow, E.F., and Qin, J. (2000). A structural basis for integrin activation by the cytoplasmic tail of the α_{IIb} subunit. Proc. Natl. Acad. Sci. USA *97*, 1450–1455.

Weljie, A.M., Hwang, P.M., and Vogel, H.J. (2002). Solution structures of the cytoplasmic tail complex from platelet integrin alpha IIb- and beta 3-subunits. Proc. Natl. Acad. Sci. USA *99*, 5878–5883.

Woodside, D.G., Liu, S., and Ginsberg, M.H. (2001). Integrin activation. Thromb. Haemost. *86*, 316–323.

Wüthrich, K. (1986). NMR of Proteins and Nucleic Acids (New York: John Wiley and Sons).

Yan, B., Calderwood, D.A., Yaspan, B., and Ginsberg, M.H. (2001). Calpain cleavage promotes talin binding to the beta 3 integrin cytoplasmic domain. J. Biol. Chem. *276*, 28164–28170.

Xiong, J.P., Stehle, T., Diefenbach, B., Zhang, R., Dunker, R., Scott, D.L., Joachimiak, A., Goodman, S.L., and Arnaout, M.A. (2001). Crystal structure of the extracellular segment of integrin alpha Vbeta3. Science *294*, 339–345.

Zhou, P., Lugovskoy, A.A., and Wagner, G. (2001). A solubility-enhancement tag (SET) for NMR studies of poorly behaving proteins. J. Biomol. NMR *20*, 11–14.

Zwahlen, C., Legault, P., Vincent, S.J.F., Greenblatt, J., Konrat, R., and Kay, L.E. (1997). Methods for measurement of intermolecular NOEs by multinuclear NMR spectroscopy: application to a bacteriophage λ N-peptide/*box*B RNA complex. J. Am. Chem. Soc. *119*, 711–721.

Accession Numbers

Coordinates of α_{IIb}/β_3 tail complex have been deposited in the Protein Data Bank with the accession code 1M8O.

Note Added in Proof

In this issue of *Cell*, a paper by Dr. Timothy Springer and his associates (Takagi, J., Petre, B.M., Walz, T., and Springer, T.A. [2002]. Cell *110*, 599–611) demonstrates global conformational change in integrin extracellular domains during integrin inside-out and outside-in signaling.